Optimizing Welding Parameters for Steam Transport Pipes Made of Stainless Steel 316 in Desalination Plants

Faisal O. Salem[1], Nuri M. Bhieh[2], Esmaileel Sughayiere [3]
eng.fos@gmail.com[1], nuri.bhieh@tpc.ly[2], esmaileelsughayiere@gmail.com[3]
Post-graduate student Libyan academic[1]
The Libyan Higher Technical Center for Training and Production[2]
Libyan Occupational Advanced Center for Welding [3]

Abstract

This study was aimed to examine effects of welding parameters on mechanical properties of Stainless Steel 316 welded joints, which were welded by Tungsten Inert Gas (TIG) welding technique. The study investigated the effects welding current and Argon flow rate on mechanical properties of the joints. Taguchi method was applied to design and optimize the experimental work of the study, and Non-destructive as well as destructive tests have been conducted to measure the mechanical properties of the welded joints. The results, clearly, shown that a current of 95A and a gas flow rate of 12 L / min, have achieved the optimum tensile strength of 592.47 MPa.

Keywords: TIG, Stainless Steels, welding current, Aargon flow rate, TIG, and Taguchi approach, Mechanical properties.

الملخص

هدفت هذه الدراسة إلى دراسة تأثير معاملات اللحام على الخواص الميكانيكية للوصلات الملحومة من الصلب المقاوم للصدأ 316 والتي تم لحامها بتقنية اللحام بالغاز الخامل (TIG). تناولت الدراسة تأثير تيار اللحام وتدفق غاز الأرجون على الخواص الميكانيكية للمفاصل. تم تطبيق طريقة تاقوشي لتصميم وتحسين التجارب العملية للدراسة، كما تم إجراء اختبارات غير إتلافيه وكذلك إتلافيه لقياس الخواص الميكانيكية للوصلات الملحومة. أظهرت النتائج بوضوح أن تيار 95 أمبير ومعدل تدفق غاز يبلغ 12 لترًا / دقيقة ، قد حققا مقاومة الشد المثلى البالغة 592.47 ميجا باسكال.

1. Introduction

Some environmental and operating factors as in Zliten desalination plant such as; higher temperatures, evaporation, higher chloride content, lower pH, and higher levels of tensile stress all require special material to deal with. That is why the use of a 316 austenitic stainless steel recommended over other materials, due to its distinct properties and excellent corrosion resistance. There are several characteristics of the family of corrosion resistant steel known as stainless steel, that make them highly desirable and highly qualified for desalination service, not only for piping applications but for all desalination plant system [1]. Stainless steels are certain alloys of iron and chromium that are highly resistant to corrosion and oxidation at high temperatures and maintain considerable strength at these temperatures.

These alloys contain nickel - chrome, and small percentages of silicon, tungsten, molybdenum, and copper, etc. [2]. Therefore, to carry heated and pressurized steam in high efficiency requires a good piping system joint with no defects during joining. Thus, welding is an important process in desalination plants. Welding is one of the major ways to fabricate metal parts. It is achieved by permanently fastening together two or more pieces into a single homogeneous part by the application of heat, pressure, or both [3]. Although there are many welding processes, three are the most important today "arc welding, gas welding, and resistance welding". Besides, the weldability of material must know, which is, depends on different factors like the metallurgical changes that occur during welding, changes in hardness in weld zone due to rapid solidification, and the extent of oxidation due to the reaction of materials with atmospheric oxygen and tendency of crack formation in the joint position. According to previous studies [5-12] related to welding of stainless steels during the past years, a lot of researches has been done on the welding of stainless steel, an agreement was observed in some studies that the most significant parameter is current as influential on weld joints, along with other welding variables such as gas flow rate, velocity, voltage, groove angle and polarity. Therefore, the welding process that would be use is Tungsten Inert Gas (TIG). Using different welding parameters for the process had studied, which affect the weld quality, such as welding current (I), voltage (V), and gas flow rate (GFR). Then by using tensile test at room temperature, where the ultimate stress that the pipe base metal withstand was 25.18 KN and the tensile strength was 537 MPa.

2. Experimental work

Pipes of type 316 austenitic stainless-steel were subjected of this research investigation. The pipes are used in Zlitan desalination plant because this type of material is recommended by standards for such conditions due to its distinct properties and excellent corrosion resistance, the pipes were collected from the plant with the required length for the study, then the chemical analysis processes have been conducted composition to know the chemical composition and to make sure the pipes are truly belonged to this type of stainless-steel family.

2.1 Chemical composition analysis

The spectrometric analysis of the specimen was conducted using Foundry Master Pro to find the chemical composition of tube base metal. As shown in the results in table 1, it is clear that the stainless steel is grade 316.

Table 1. Chemical composition of tube material

Element	C	Cr	Si	Ni	Mo	Nb	Ti	Mn	Fe	V
Wt. %	0.088	17.1	0.593	12.4	2.41	0.042	0.006	0.792	64.9	0.0562

2.2 Cutting

A pipe of 90 mm diameter and 4mm thick, was cross-sectionally cut into 20 pieces of 130 mm length each. An inox pipe cutting saw was used to do this task.

2.3 Lathing

The pipe thickness was checked to determine the appropriate groove dimensions, which were determined according to standard "ISO, 9692-1:2013" [4]. A lathe machine and tool of carbide-insert type were used to machine the pipe face and make the proper chamfer on the pipe's edge as shown in Figure 1. The chamfer was intended to make the grove when the pipe assembled with another pipe before welding. A single-V-groove design of 60º angle and 2 mm root face (s) shown in figure 1 was selected. A gape of g = 1.4 to 2 mm length between the two adjacent pipes was left to be filled by welding.

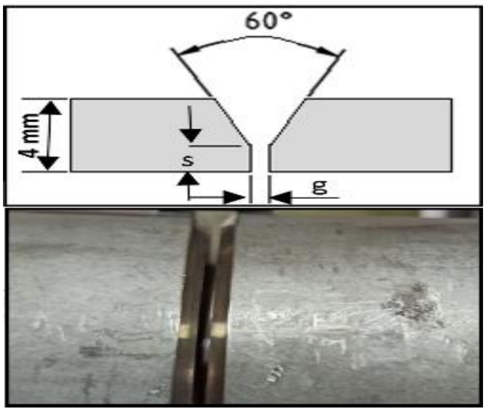

Figure 1. Design of joint

2.4 Cleaning

Two processes were used to clean the samples, a mechanical process to remove the impurities from a metal's surface, and a chemical one that deepened on solvents and acids to remove paint, oil, and grease.

2.5 Welding

The TIG welding process was used in order to weld metal 316, with changing the parameters suitable for welding process. 10 pairs (20 pipes) of 316 stainless steel samples were welded together to make samples of 260 mm length. Table 2 illustrates the general information of the samples and table 3 illustrates the experimental setup beside the ranges of current and gas flow have been applied in the experiments.

Table 2. Specimen general information

Specimen Parameter	Pipe thickness	Pipe material	Outer diameter	Internal diameter	Number of pieces	Number of pairs	Filler metal type	Filler metal diameter	Type of joint
Value	4 mm	316 stainless steel	90 mm	82 mm	10 pieces	5 pairs	316 L	1.6 mm for 1st pass 2.4 mm for 2nd pass	Butt joint V Shape 60-degree edges

Table 3. TIG parameters

Expert No.	Current I (Amp)	Gas flow rate GFR (L/min)	Polarity	Filler rods	Shielding gas	Voltage
1.1	95	12	DCEN	316 L	Argon	Rated 18 – 22 volt
1.2	95	14				
1.3	95	16				
1.4	105	14				
1.5	105	16				
1.6	105	12				
1.7	115	16				
1.8	115	12				
1.9	115	14				

The circular pipe was divided into two parts as shown in figure 2; one side was from 0º to 180º, and the other side was from 180º to 360º for whole samples. By applying different parameters for each side. By using two fittings at the angles (0° to 180°) of the pipe, then the pipe was placed on a 90° edged sheet metal, and clamp it with two clamps to make the two parts stables, as shown in figure 2.

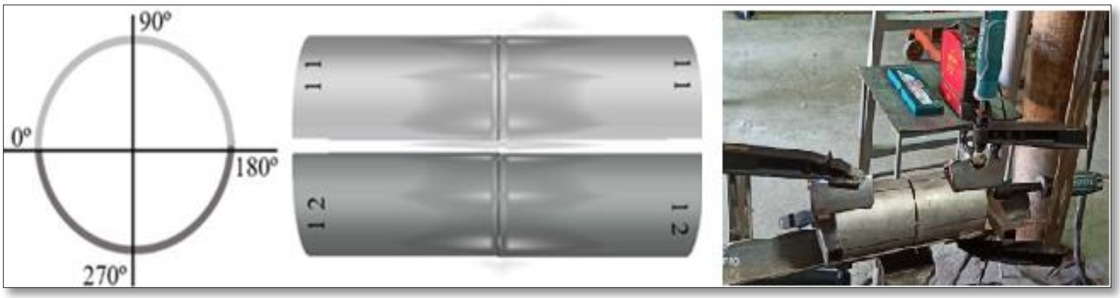

Figure 2. Welding procedure

The parameters which chosen to use are shown in the above tables 2 and 3, are current and shielding gas flow according to the sample number. Where the other variables kept constants as:

- Filler metal which we used is stainless steel 316L, the diameter of the first pass is 1.6 mm and the second pass is 2.4 mm.
- The polarity used is direct current electrode negative "DCEN".
- The voltage is in range between 18 to 22 depending on the arc distance.
- Purging gas is argon with a flow rate 10 L / min,.

A purging process used to remove the oxygen from the inside part of the pipe to protects the back of the weld from oxidation due to the high heat of TIG welding. An argon gas was used, because argon less expensive than helium. The purging gas flow rate which used is 10 L / min, the purging gas flowing was kept for a time to fill the chamber before starting weld, also the purging gas flow was continuing during the welding, this means that air can’t get back into the purge zone. The figure 3 demonstrates the purging process.

Figure 3. Purging gas in TIG

2.6 Inspection

2.6.1 Vision

It is economical and fast process to check (by man eyes) the welding quality, and catch any of the external defects such as :

- Distortion of the workpiece
- Unfilled grove
- Surface porosity
- Undercut
- Overlap
- Incomplete penetration
- Improper shape of weld profile

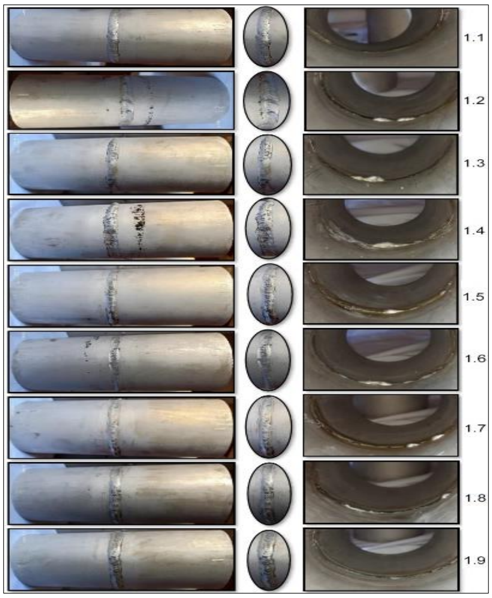

Figure 4. Vision inspection of specimen

2.6.2 X-Ray Radiography

X-Ray Radiography test was conducted to determine the welding internal defect such as porosity, internal incomplete welding, lack of fusion, and slags. The X-ray radiographic inspection machine of type “88144 SMART ANDREX 225KV” was used and its setting is shown in table 4.

Table 4. X-Ray radiography setting

X-ray radiographic inspection setting	
Curies / KV & mA	200 KV, 3 mA
Exposure time	20 sec
Penetration thickness	4 mm
IQI type & designation	6 FEEN
Development time	5 min
Focal spot / source size	3*3 mm
Film type	D7
Screen - type & thickness	Pb 2*0.1 mm

2.7 Milling

Milling processes was conducted in two stages:

2.7.1 Cutting longitudinal strips

The welded pipes were placed on the table of the milling machine, and fixed from two sides, then they were longitudinally cut into strips of 25 to 30 mm width of each sample. The milling machine shown in figure 5 was used to cut the samples, and the tool was an endmill made of carbide. The milling speed was high and feed rate was low. To dissipate the heat arose during the milling operation, a lubricant was applied all the time of milling.

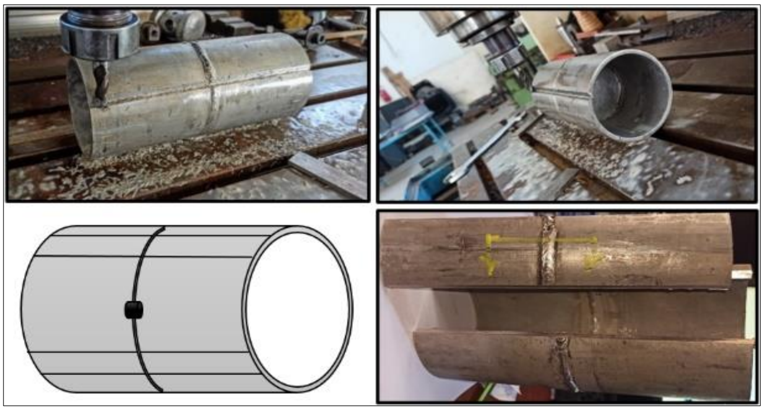

Figure 5. Cutting longitudinal strip by milling

2.7.2 Making tensile test specimens out of the strips

The second stage is to machine the longitudinal strips into a tensile test-shape samples using the milling machine as illustrated in figures 6 and 7, the milling speed of machine was medium and feed rate was low, the lubricant was continuously applied during the milling. Because the tool was made of steel. The average working time of each sample 180 min. the specimens' dimensions were selected based on the Standard E8/E8M -16A as shown in figure 6.

	Specimen 1
	mm [in.]
G—Gauge length	50.0 ± 0.1 [2.000 ± 0.005]
W—Width	12.5 ± 0.2 [0.500 ± 0.010]
T—Thickness	
R—Radius of fillet, min	12.5 [0.5]
A—Length of reduced parallel section, min	60 [2.25]
B—Length of grip section, min	75 [3]
C—Width of grip section, approximate	20 [0.75]

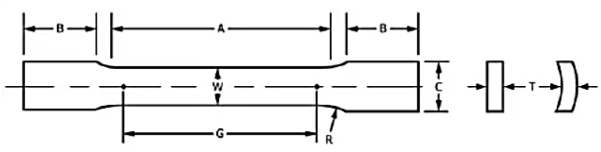

Figure 6. Standard of tensile specimen

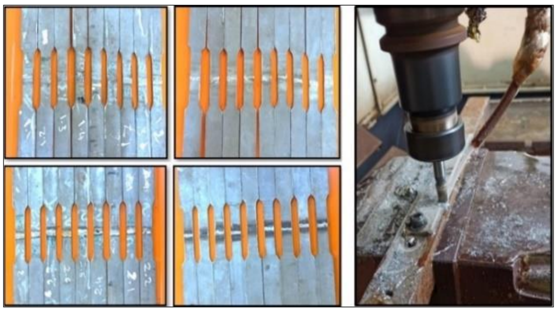

Figure 7. Formed tensile strength specimens

2.8 Manually grinding

In this process, the samples were cleaned using emery papers to remove all machining chips in order to be able to measure the dimensions of the samples accurately.

2.9 Cross-sectional area calculations

The area exposed to tensile stress is shaded in Figure8, and it must be calculated as follow.

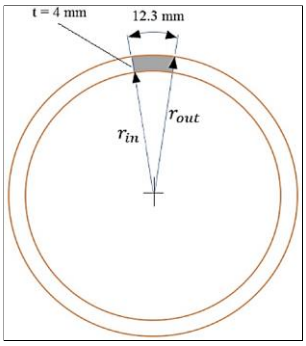

Figure 8. Drawing of the used area in tensile strength equation

To calculate the arc length (L),

$$(\mathrm{L}) = \frac{\theta}{360} * (2 * \pi * r) \ldots \ldots \ldots \ldots \ldots \ldots \ldots \ldots \ldots \ldots \ldots \ldots \ldots \ldots \ldots \ldots \ldots \ldots \ldots \ldots \ldots (1)$$

Where $\theta = \frac{12.3*360}{(2*3.142*45)} \quad \Rightarrow \quad \theta = 15.668°$

Same angle and same equation except the angle are known but length of arc is unknown.

$$\because \ L\,arc = \frac{\theta}{360} * (2 * \pi * r)$$

$$L\,arc = \frac{15.66}{360} * (2 * 3.142 * 41) \qquad \therefore \ L\,arc = 11.20\,mm$$

The cross-sectional (As) of every specimen was calculated using equation (2) as following:

$$As = \left(\frac{\theta}{360} * (\pi * r_{out}^2)\right) - \left(\frac{\theta}{360} * (\pi * r_{in}^2)\right) \ldots \ldots \ldots \ldots \ldots \ldots \ldots \ldots \ldots \ldots \ldots \ldots \ldots \ldots . (2)$$

$$As = \left(\frac{15.66}{360} * (3.142 * 45^2)\right) - \left(\frac{15.66}{360} * (3.142 * 41^2)\right) \qquad \therefore \ As = 47.02\,mm^2$$

Following the same calculations approach, the cross-sectional areas of specimens were slightly different as shown in table 5

Table 5. Cross-sectional areas of all specimens

Numbe	Area mm^2
1.1	47.02
1.2	47.18
1.3	47.09
1.4	46.82
1.5	47.15
1.6	47.19
1.7	47.22
1.8	46.87
1.9	47.41

3. Results and Discussion

3.1 Results of Visual Inspection

Table 6 demonstrates the results of visual inspection for TIG specimens. Specimens 1.1, 1.4, and 1.8 have overlap defects. The rest of specimens have no visual defects.

Table 6. Results of visual inspection

Specimen No.	Type of defect	Comment
1.1	**-**	**Excessive weld**
1.2	**-**	**-**
1.3	**Porosity**	**-**
1.4	**-**	**Excessive weld**
1.5	**-**	**-**
1.6	**-**	**-**
1.7	**-**	**-**

1.8	**-**	**Excessive weld**
1.9	**-**	**-**

3.2 Results of X-ray radiography tests

All results of radiographic inspection are described in table 7, the porosity found in sample 1.3 with a current of $95A$ and gas flow rate $16\ L\ /\ min$, where the rest of specimens looks clear.

Table 7. X-Ray Radiography results

Specimen No.	Distortion of the workpiece	Unfilled cavity and porosity	Undercut and overlap	Incomplete penetration
1.1	no	no	overlap	no
1.2	no	no	no	no
1.3	no	no	no	no
1.4	no	no	overlap	no
1.5	no	no	no	no
1.6	no	no	no	no
1.7	no	no	no	no
1.8	no	no	overlap	no
1.9	no	no	no	no

3.3 Results of tensile tests

Table 8 lists the results of tensile test results. It was observed that the specimen 1.1 (current of $95\ A$ and gas flow rate of $12\ L\ /\ min$). As shown the highest tensile stress of $592.47\ MPa$.

Table 8. Tensile strength tests results

Specimen No.	GFR L/min	I Amp	A mm^2	US N	TS MPa
1.1	12	95	47.02	27,858	592.47
1.2	14		47.18	26,352	558.54
1.3	16		47.09	27,176	577.11
1.4	14	105	46.82	27,441	586.1
1.5	16		47.15	27,350	580.06
1.6	12		47.19	25,411	538.48
1.7	16	115	47.22	27,705	586.72
1.8	12		46.87	27,705	591.1
1.9	14		47.41	28,058	591.82

The stress-strain curve of sample 1.1 shows the load increase from zero to ultimate stress that the sample withstand 27.85 KN, before dropping almost vertically, and the displacement increases from zero to a little over 40 mm, the sample has been broken in the base material far from the weld center as shown in the figure 9.

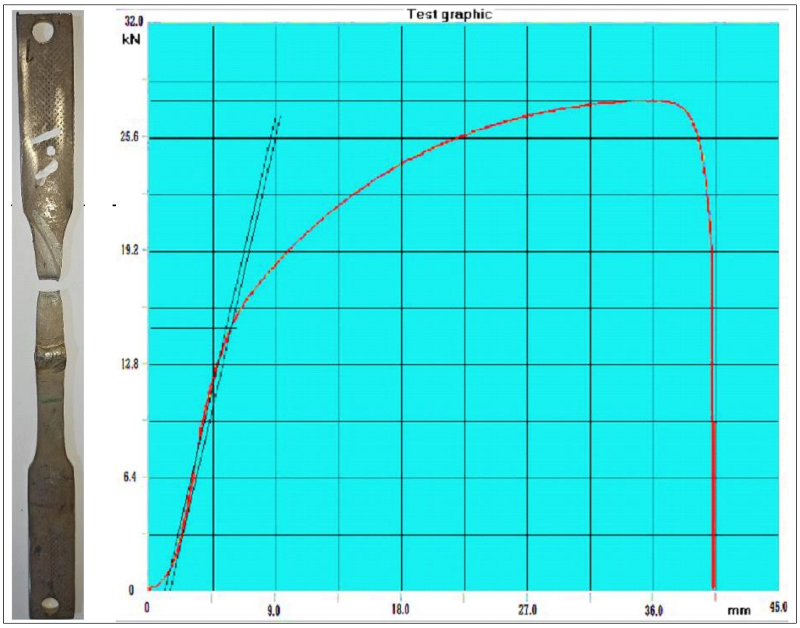

Figure 9. Shape of specimen 1.1 after the test and its stress-strain curve

4. Results analysis

This section analyzes the tensile test results of this study. Figure 10 shows the effect of welding current and gas flow rate on tensile stress of the specimens. The figure shows that the highest tensile stress was 592.47 MPa when the current was 95 A and the gas flow rate was 12 $L\ /\ min$ (specimen 1.1).

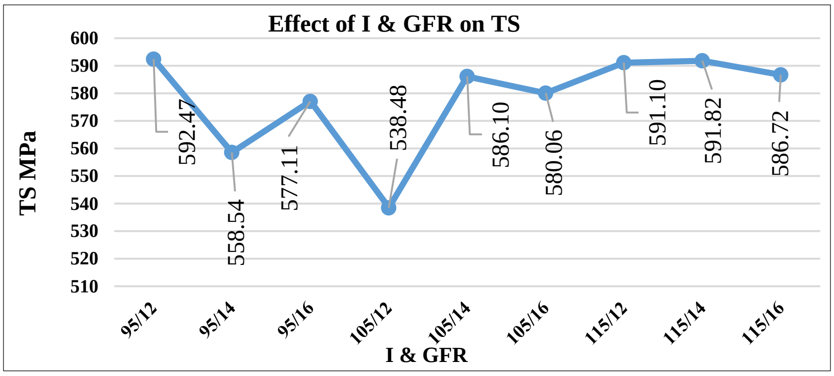

Figure 10. Effect s of I & GFR on TS

On the other hand, the most stable results were observed with differences in gas flow rate at current 115 A, where the tensile stress was close to each other. As it was also observed that all specimens welded by TIG have a tensile stress greater than the tensile stress of the base metal.

4.1 Analysis Using Taguchi approach

An orthogonal array was designed using Minitab17 depending on Taguchi approach, where the welding current vs gas flow rate were used to calculate S/N ratio. The array design L9 (3*2), and the levels are three levels for both processes as shown in illustrated table 9.

Table 9. Design of experiments

Welding parameter	Level		
	1	2	3
Current Amp	95	105	115
Gas flow rate L/min	12	14	16

By using the analyze of Taguchi design for tensile strength as a response factor and the S/N ratio as the large is better.

4.2 Taguchi analyzing

In order to obtain the optimal welding conditions, the larger is the better is used as the S/N ratio of quality characteristic as shown at table 10. As demonstrated in these results, the main effects plot for S/N ratio indicates that current which has the largest effect on the S/N ratio. On average, experimental runs with current 115 Amp had much higher S/N ratios 55.42 than experimental runs with current 105 Amp which had a small effect on the S/N ratio 55.08 as showing in figures 11 and 12.

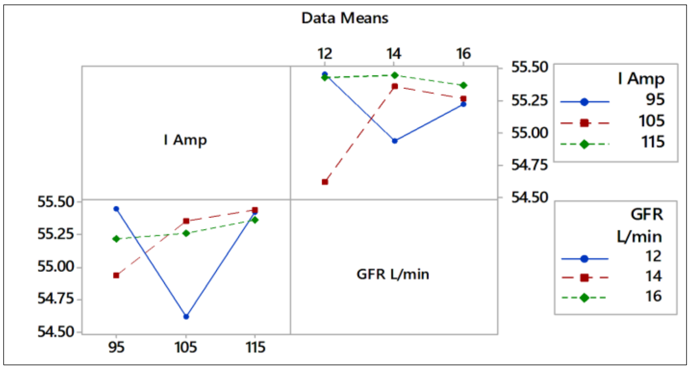

Figure 11. Interaction plot for S/N ratios

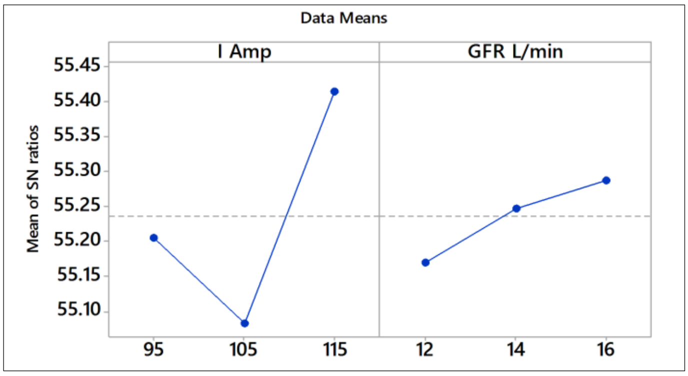

Figure 12. Main effect plot for S/N ratio

For Taguchi analysis were TS MPa vs I Amp and GFR L/min. Response tables 11 and 12 for S/N ratios larger is better; According to ranks in a response table, the factor with the largest delta value is current it's given the 1st rank, then the factor with the less delta value is gas flow rate it's given the 2nd rank. While delta shows the difference between the highest and lowest characteristic average for a factor.

Table 11. Response values for S/N

Level	I Amp	GFR L/min
1	55.21	55.17
2	55.08	55.25
3	55.42	55.29
Delta	0.33	0.12
Rank	1	2

Table 12. Response values for means

Level	I Amp	GFR L/min
1	576.0	574.0
2	568.2	578.8
3	589.9	581.3
Delta	21.7	7.3
Rank	1	2

The figure 13, a contour plot shows the potential relationship between three variables current, gas flow rate, and tensile strength. A contour plot is like a topographical map in which x-, y-, and z-values are plotted instead of longitude, latitude, and elevation.
The darker regions identify higher tensile strength values. The contour levels reveal a peak centered in the vicinity of 13.5 to 15.5 of (GFR) and 105 to 115 of (I). Also, the quality scores in this peak region are greater than 590 MPa.

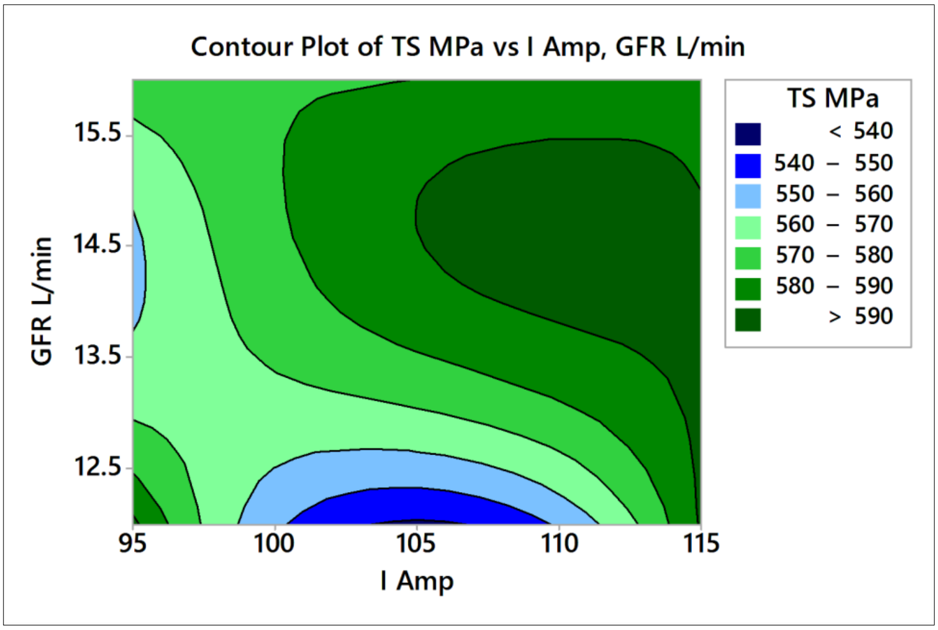

Figure 13. Contour plot of TS vs I, GFR

5 Conclusion

In this study the tensile strength of welded specimens by using TIG welding process, where the welding current and gas flow rate response to tensile strength in TIG process.
Through the results obtained after conducting destructive and non-destructive tests on the welded specimens of the tube made of stainless steel 316. It was observed that the most influential variable for both welding processes is current.

- The highest tensile strength was obtained $592.47\ MPa$. when the current is 95 A, and the gas flow rate is $12\ L\ /\ min$,
- All specimens have slightly higher tensile strength than the tensile strength of the base metal of the used tube.
- The visual inspection shows that all TIG specimens have no defects such as distortion, unfilled cavity, and incomplete penetration. Except the specimens 1.1, 1.4, and 1.8 have an overlap defect.
- All X-ray radiography inspection of TIG specimens has no porosity occurred, except specimen 1.3 with a current of 95 A and gas flow rate of $16\ L\ /\ min$.

References

[1] H. W. Yankee, Manufacturing processes, USA: Prentice-Hall, 1979.

[2] Khan, Md. Ibrahm, Welding science and technology, New age international publishers, 2007 .

[3] "ESAB," [Online]. Available: https://www.esabna.com/euweb/mig_handbook/592mig4_4.htm.

[4] ISO, "International standard," vol. second edition, no. 9692-1:2013(E), p. 3, 2013.

[5] Halil Ibrahim Kurt, Ramazan Samur, "Study on Microstructure, Tensile Test and Hardness 304 Stainless Steel Jointed by TIG Welding," International Journal of Science and Technology, vol. 2, pp. 163 - 168, 2013.

[6] Navid Moslemi, Norizah Redzuan, Norhayati Ahmad, Tang Nan Hor, "Effect of Current on Characteristic for 316 Stainless Steel Welded Joint Including Microstructure and Mechanical Properties," ELSEVIER, pp. 560 - 564, 2015.

[7] Devendran, Sujay, Sangamithirai, Mohamed Thameem, Hari Kumaraan, "Analyzing the Parameters of SS 304 using TIG Welding," International Research Journal of Advanced Engineering and Science, vol. 2, no. 2, pp. 290 - 294, 2017.

[8] P. P. Thakur, A. N. Chapgaon, "A Review on Effects of GTAW Process Parameters," IJRASET, vol. 4, no. I, pp. 136 - 140, 2016.

[9] Nirmalendhu Choudhury, Ramesh Rudrapati, Asish Bandyopadhyay, "Design optimization of Process Parameters for TIG Welding based on Taguchi Method," International Journal of Current Engineering and Technology, no. 2, pp. 12 - 16, 2014.

[10] S. M. Ahir, N. B. Patel, K. A. Patel, "Expermental investigation of welding distortion of austenitic stainless steel 316 in TIG wlding," IJEDR, vol. 3, no. 2, pp. 781 - 785, 2015.
[11] Vijay Gohel, Jatin Makwana, Riteshkumar Ranjan, "Optimization of process parameter for tensile strength and hardness of S.S 304 by TIG welding," IJEDR, vol. 4, no. 2, pp. 756 - 760, 2016.
[12] P. Bharath, V.G. Sridhar, M. Senthil kumar, "Optimization of 316 Stainless Steel Weld Joint Characteristics using Taguchi Technique," Elsevier, pp. 881 - 891, 2014.
[13] ASTM, "Standard Test Methods for Tension Testing of Metallic Materials," vol. E8/E8M, pp. 10 - 11, 2013.